

SiC Nano-Dots in Bulk-Si Substrate Fabricated by Hot-C⁺-Ion Implantation Technique

T. Mizuno, S. Nakada, M. Yamamoto, S. Irie, Y. Omata, T. Aoki, and T. Sameshima*

Kanagawa Univ., Hiratsuka, Japan (mizuno@info.kanagawa-u.ac.jp), * Tokyo Univ. of Agric. and Tech., Koganei, Japan

Abstract

We experimentally studied SiC nano-dot formation in a bulk-Si substrate to realize the strong photoluminescence (PL) intensity I_{PL} for a future Si-photonic device, using the very simple processes of a hot-C⁺-ion implantation (HCl) into Si substrate and the following N₂ annealing (NA). We confirmed the 3C/4H-SiC nano-dots with approximately 5-nm diameter L in the C-rich layer (CRL) near surface-oxide (SOX)/Si interface. In addition, the I_{PL} strongly depends on the NA temperature T_N , and successfully optimized both the HCl temperature T and T_N to achieve the strong I_{PL} in the near-UV/visible regions.

I. Introduction

Recently, we experimentally studied a Si_{1-y}C_y layer fabricated by the HCl into a (100)SOI at $T=900^\circ\text{C}$ in a wide range of $0.01 < Y \leq 0.25$ and $0.5 \leq d_S \leq 20\text{nm}$, where d_S is the SOI thickness [1], [2]. We demonstrated very large bandgap E_G ($\approx 3\text{eV}$) (peak-wavelength λ_{PL} of 400nm) and strong PL emission of the Si_{1-y}C_y layer in the near-UV/visible regions ($> 400\text{nm}$), which drastically increases with increasing Y in $Y \leq 0.25$. C atoms segregate at both the SOX/Si and buried-oxide BOX/Si interfaces, resulting in the partial formation of 3C-SiC in a C segregation layer (CSL) near the BOX/Si interface [2]. Strong I_{PL} , which is approximately 100 times as large as that of 2D-Si [2], is mainly emitted from the CSL. Thus, the Si_{1-y}C_y technique is very suitable for both visible Si-based photonic devices [3] as well as novel E_G engineering for high-speed source-heterojunction devices (SHOT) [4]. On the other hand, it is reported that SiC nanoparticles are synthesized by the chemical vapor phase method and the E_G increases with decreasing the dot diameter L obeyed by the quantum confinement effects (QCE), and in addition, the E_G of 4H-SiC is larger than that of 3C-SiC [5].

In this work, we experimentally studied SiC nano-dot formation in a (100) bulk-Si substrate for future Si-based photonic devices, using the simple process of HCl and the following NA. We confirmed very strong PL emission from the SiC nano-dots, which is about 5 times as large as that from the C⁺ implanted SOI [2].

II. Experiment Procedure

SiC nano-dots were fabricated by the simple processes of the HCl into (100) bulk-Si substrate with 100-nm-thick SOX layer (Fig.1(a)) at two T conditions of 600 or 800°C (Fig.1(b)) and the following NA in various T_N (Fig.1(c)), where the C⁺ ion dose D_C was $4 \times 10^{16}\text{cm}^{-2}$ [2], $500 \leq T_N \leq 1200^\circ\text{C}$, and the NA time t_N was 10min. We also fabricated 20-nm thick SOI [2] substrates fabricated by the same HCl conditions without NA, as a reference.

The material structures of the C-rich layer (CRL) near the SOX/Si interface was evaluated by corrector-spherical aberration TEM (CSTEM) and the electron diffraction (ED) patterns obtained by fast-Fourier-transform (FFT) analysis of the lattice spots. The C content Y depth profile was evaluated by the C1s spectrum of XPS. PL properties before and after NA were measured at room temperature, where the excitation laser energy E_{EX} was 3.8eV and the laser diameter was 1μm. At $E_{EX}=3.8\text{eV}$, the PL photons were mainly emitted from the surface SiC nano-dots in the CRL, because the photon penetration length of 3.8eV laser in Si is only 8.7nm [2]. The PL spectrum in a wide range of photon wavelengths from the UV to NIR region was calibrated using a standard illuminant.

III. Results and Discussions

A. SiC Nano-Dot Formation

The Y depth profiles of the Si-C bond, obtained by the C1s spectrum, shows that the C atoms are also segregated at the SOX/Si interface and the Y is higher than 10 at.% within 30-nm depth from the Si surface in CRL (Fig. 2). However, the Y profile of the bulk-Si is much different from that of SOI (dotted line in Fig.2), and thus, the peak Y of bulk-Si (=0.13) is about one half of that of SOI (=0.25).

As a result, CSTEM observations show that many SiC dots are successfully formed in the CRL from the Si-surface to the depth of about 50nm (Fig.3), where $D_C=4 \times 10^{16}\text{cm}^{-2}$, $T=800^\circ\text{C}$, and $T_N=900^\circ\text{C}$. The L is varied from approximately 3 to 7nm, and the dot density N_D is estimated to be approximately $4.6 \times 10^{18}\text{cm}^{-3}$ which is about 1000 times as large as that of SOI substrate without NA.

Thus, the high N_D is considered to be caused by the C atom clustering effects [6] in the bulk-Si during the NA. Thus, the SiC nano-dot (zero-dimension (0D)) causes the large band-structure modulation caused by QCE, which results in the larger I_{PL} and higher E_G of SiC dots. In addition, CSTEM observation shows that two types of 3C/4H-SiC dots were formed (Figs. 4(a) and (c)). The ED patterns show the interference by the two layers of SiC and Si (Figs. 4(b) and (d)). The SiC-dots are divided into two types of 3C-SiC dot (Fig.4(b)), and 4H-SiC dot (Fig. 4(c)). The N_D of 4H-SiC dot; N_D^{4H} is higher than that of 3C-SiC dot; N_D^{3C} , where the E_G of 4H-SiC dot (E_{4H}) is higher than that of 3C-SiC dot (E_{3C}) [5]. Moreover, 3C-SiC dots were also formed at the CSL [2]. Thus, two types of SiC nano-dots coexist in the CRL near the Si surface (Fig. 5). Measured PL spectrum is expected to be the sum of the PL from the three regions of I_H (4H-SiC), I_M (3C-SiC), and I_L (Si_{1-y}C_y).

B. T_N Dependence of PL Properties

SiC nano-dots before NA can emit PL photons from the near-UV to visible regions. The PL spectra in the bulk-Si and SOI are divided into three types; Type-I ($I_H \approx I_M$) with $\lambda_{PL} \approx 480\text{nm}$ ($E_{PH} \approx 2.5\text{eV}$) at $T=800^\circ\text{C}$, Type-II ($I_H \approx I_M$) with a double λ_{PL} in SOI [2], and Type-III ($I_H > I_M$) with $\lambda_{PL} \approx 400\text{nm}$ ($E_{PH} \approx 3.1\text{eV}$) at $T=600^\circ\text{C}$ (Fig. 6). In addition, Type-I drastically changes after NA, and the I_{PL} in both types strongly depends on T_N and has the maximum value at $T_N \approx 900^\circ\text{C}$ (Figs.7). Especially, at $T=600^\circ\text{C}$ (Fig. 7(b)), the I_{PL} enhancement after NA extends to approximately 3.6, but the spectrum type of III is independent of T_N . However, the Type-I at $T=800^\circ\text{C}$ changes into Type-III in $T_N < 1200^\circ\text{C}$ (Fig. 7(a)).

All PL spectra can be well fitted by three components of Gaussian carves I_H with high E_{PH} (E_H), I_M with middle E_{PH} (E_M), and I_L with low E_{PH} (E_L) (for examples in Fig.8), which suggests that the PL emission layer consists of three different E_G materials of the 3C-/4H-SiC dots, and the Si_{1-y}C_y, as expected (Fig.5). Thus, the PL spectrum type can be explained by the ratio R_C of I_H and I_M ($\equiv I_H/I_M$), that is, the polytype of SiC (3C or 4H). Thus, Type-III has stronger I_H (Fig.8). At $T_N=900^\circ\text{C}$, the Type-I spectrum at $T=800^\circ\text{C}$ before NA is transferred into a type-III after NA (Fig.7(a)), because of the rapid increase of I_H after NA.

Here, we summarize the T_N dependence of each E_{PH} (λ_{PL}) and I_{PL} (Figs.9 and 10). Each E_{PH} , that is, each peak- λ_{PL} slightly depends on T_N (Fig.9). In addition, the E_H and E_M values are close to the theoretical expanded E_G values; E_{4H} and E_{3C} of $L=2\text{nm}$ nano-dots [5], respectively. Thus, I_H and I_M are probably emitted from the 4H and 3C nano-dots (Figs.4), respectively. E_M at $T=600^\circ\text{C}$ is higher than that at $T=800^\circ\text{C}$, which probably relates to the smaller L at $T=600^\circ\text{C}$, because of $E_G \propto L^{-2}$ [5].

On the other hand, the I_{PL} has the maximum value at $T_N \approx 900^\circ\text{C}$. The I_{PL} enhancement factors at T of 600 and 800°C , compared to I_{PL} of SOI, extend to 4.4 and 1.9, respectively (Figs.10). The large I_{PL} enhancement is mainly attributable to the larger I_H enhancement factors of 3.3 at $T=600^\circ\text{C}$ and 2.9 at $T=800^\circ\text{C}$, which indicates that the N_D^{4H} drastically increases after NA. In addition, at $T=600^\circ\text{C}$, the R_C is higher than 1, that is $N_D^{4H} > N_D^{3C}$. However, the R_C at $T=800^\circ\text{C}$ is lower than 1 ($N_D^{4H} < N_D^{3C}$) except at $T_N = 900^\circ\text{C}$ (Fig.10(c)). Thus, the PL spectrum type can be explained by the R_C . Therefore, the NA process is very suitable for improving I_{PL} . Consequently, the N_D , L , and R_C of SiC dots can be controlled by T and T_N , which leads to the PL intensity improvement and the peak- λ_{PL} (color) control in a future Si-based photonic device.

IV. Conclusion

We experimentally demonstrated 3C-/4H-SiC nano-dot formation in a bulk-Si substrate, using the combination of HCl and the following NA processes. The PL intensity drastically increases after the NA. The peak λ_{PL} (emission color) and intensity can be controlled by T , T_N , and R_C by optimizing the process. Thus, the SiC-dot technology is very promising for future photonic devices.

Acknowledgement: This work was partially supported by KAKENHI (17K06359).

References: [1] T.Mizuno, JJAP **55**, 04EB02, 2016. [2] T.Mizuno, JJAP **56**, 04CB03, 2017. [3] S. Saito, IEDM 2008, Paper 19.5. [4] T.Mizuno, JJAP **50**, 010107, 2011. [5] J.Fan, *Silicon Carbide Nanostructures* (Springer), 2014. [6] Y.Shimizu, APL **98**, 232101, 2011.

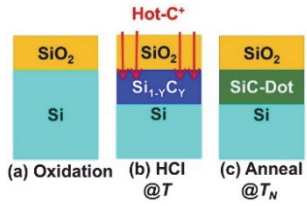


Fig.1 Fabrication steps for SiC nano-dots. (b) Hot-C⁺-ion implantation into (100)bulk-Si substrate for forming a Si_{1-x}C_x layer at T after (a) thermal oxidation of Si (≈ 100 nm). (c) N₂ annealing in various T_N was carried out to form SiC nano-dots in the bulk-Si layer.

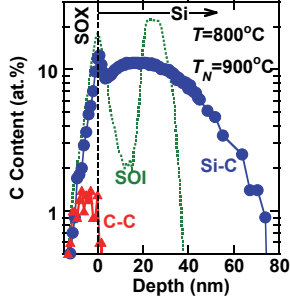


Fig.2 XPS analysis (C1s spectrum) for C content of the Si-C (circles) and C-C bonds (triangles) in the Si_{1-x}C_x layer vs depth from the Si surface, where $D_C=4\times 10^{16}\text{cm}^{-2}$, $T=800^\circ\text{C}$, and $T_N=900^\circ\text{C}$. Dotted line shows the C content of Si-C bond in 20nm-SOI before NA and the second peak shows the C segregation at BOX interface, where $D_C=4\times 10^{16}\text{cm}^{-2}$, and $T=900^\circ\text{C}$.

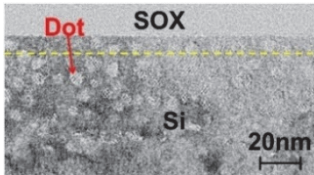


Fig.3 TEM images of the cross section of the C⁺ ion implanted Si layer, where $D_C=4\times 10^{16}\text{cm}^{-2}$, $T=800^\circ\text{C}$, and $T_N=900^\circ\text{C}$. Many SiC dots were successfully formed, as shown by the arrow. Dashed line shows the photon penetration depth of 3.8eV laser from the Si surface.

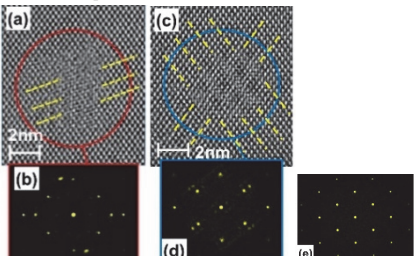


Fig.4 CSTEM images of the cross section of two types of the multilayer dots; (a) 3C-dot of [110]3C-SiC/Si with the tiled [111]-crystal-direction ($\theta\sim 36^\circ$) (dashed lines) and (c) 4H-dot with a moiré pattern of [2110]4H-SiC/[110]Si, where $D_C=4\times 10^{16}\text{cm}^{-2}$, $T=800^\circ\text{C}$, and $T_N=900^\circ\text{C}$. (b), (d), and (e) show the multilayer ED patterns (yellow dots) of the areas inside the circles in (a), (c), and Si layer, respectively. At the SOX/Si interface, the 3C-SiC dots were also observed. θ in (a) varies in each Dot-3C.

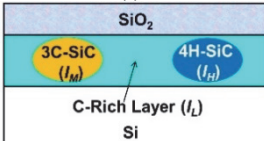


Fig.5 Schematic cross section of the bulk-Si surface. 3C- and 4H-SiC nano-dots coexist in the C-rich layer near the SOX/Si interface. It is expected that 4H-, 3C-SiC dots, and the Si_{1-x}C_x in C-rich area except SiC-dots can emit PL photons of I_H , I_M , and I_L , respectively.

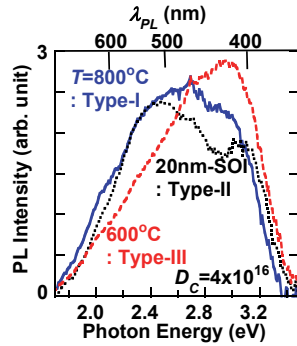


Fig.6 Three types of PL spectra of SiC in bulk-Si (bulk-SiC) at $T=800^\circ\text{C}$ (Type-I: solid line) and 600°C (Type-III: dashed line) before NA, where $D_C=4\times 10^{16}\text{cm}^{-2}$ and $E_{EX}=3.8\text{eV}$. As a reference, dotted line (Type-II) shows the result of SiC layers in SOI (SOI-SiC) before NA at $D_C=4\times 10^{16}\text{cm}^{-2}$, $T=800^\circ\text{C}$ and $d_S=20\text{nm}$. Lower and upper axes show the E_{PH} and λ_{PL} , respectively. I_{PL} of bulk-SiC is almost the same as that of SOI-SiC, but the PL spectrum type of bulk-SiC depends on T .

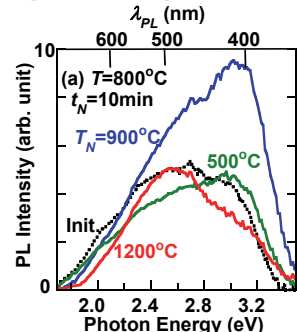


Fig.7 T_N dependence of PL spectra of bulk-SiC at (a) $T=800^\circ\text{C}$ and (b) 600°C , where $t_N=10\text{min}$ and $D_C=4\times 10^{16}\text{cm}^{-2}$. Dotted lines show the initial PL data before NA ($t_N=0$). The PL spectrum strongly depends on T_N . The optimum T_N is about 900°C to realize higher I_{PL} .

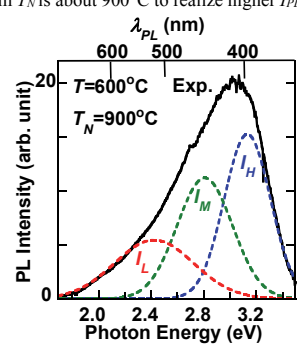


Fig.8 Gaussian curve fitting for PL spectrum after NA at $T=600^\circ\text{C}$, where $T_N=900^\circ\text{C}$, $t_N=10\text{min}$, and $D_C=4\times 10^{16}\text{cm}^{-2}$. PL spectra can be well fitted by three curves of I_H , I_M , and I_L which have high (E_H), middle (E_M), and low (E_{PH} (E_L)) shown in Fig.5, respectively, resulting in $I_H>I_M$ of Type-III.

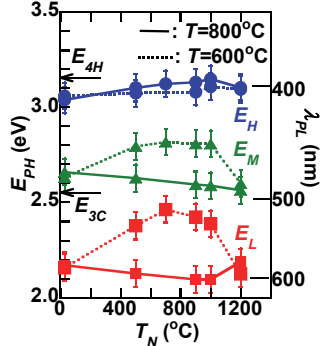


Fig.9 T_N dependence of E_H (circles), E_M (triangles), and E_L (squares) at $T=800^\circ\text{C}$ (solid lines) and $T=600^\circ\text{C}$ (dotted lines), where $t_N=10\text{min}$ and $D_C=4\times 10^{16}\text{cm}^{-2}$. The right vertical axis shows the peak λ_{PL} . The data at $T_N=25^\circ\text{C}$ show the results before NA. E_H is almost independent of T_N , but E_M and E_L have the maximum values at $T_N\approx 700^\circ\text{C}$. Arrows show the theoretical E_G of nano-dots of 3C- (E_{3C}) and 4H-SiC (E_{4H}) at $L=2\text{nm}$, respectively [5].

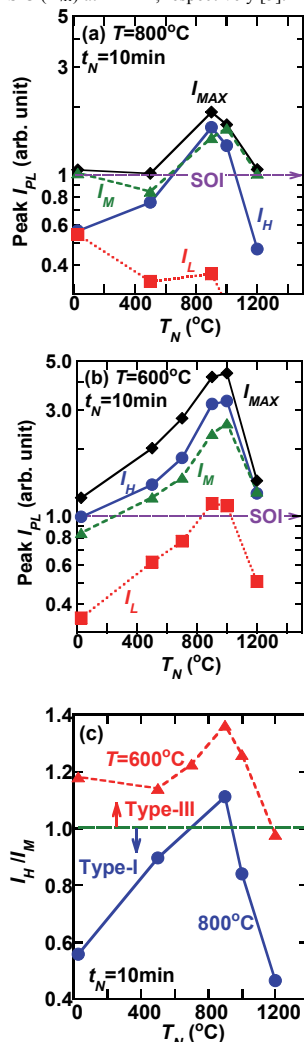


Fig.10 T_N dependence of maximum I_{PL} (I_{MAX}) (rhombi), and a peak- I_H (circles), I_M (triangles), and I_L (squares), which are normalized by the I_{MAX} value of SOI before NA at $T=800^\circ\text{C}$, where $t_N=10\text{min}$ and $D_C=4\times 10^{16}\text{cm}^{-2}$. (a) $T=800^\circ\text{C}$, and (b) $T=600^\circ\text{C}$. The data at $T_N=25^\circ\text{C}$ show the results before NA. All peak PL intensities have the maximum value at T_N of about 900°C . (c) I_H/I_M vs T_N , where circles and triangles show the data at $T=800^\circ\text{C}$ and 600°C , respectively. Type-I or III spectrum can be realized in the conditions of $I_H/I_M<1$ ($N_D^{4H}<N_D^{3C}$) or ≥ 1 ($N_D^{4H}>N_D^{3C}$), respectively.